Consistency evaluation of tropospheric ozone from ozonesonde and IAGOS aircraft observations: vertical distribution, ozonesonde types and station-airport distance

Honglei Wang[1, 2], David W. Tarasick[3*], Jane Liu[2*], Herman G.J. Smit[4], Roeland Van Malderen[5], Lijuan Shen[6], Romain Blot[7], Tianliang Zhao[1]

[1] China Meteorological Administration Aerosol-Cloud and Precipitation Key Laboratory, Nanjing University of Information Science and Technology, Nanjing, 210044, China

[2] Department of Geography and Planning, University of Toronto, Toronto, M5S 3G3, Canada

[3] Environment and Climate Change Canada, 4905 Dufferin Street, Downsview, M3H 5T4, Canada

4 Institute for Energy and Climate Research: Troposphere (IEK-8), Research Centre Juelich (FZJ), Juelich, Germany

[5] Royal Meteorological Institute of Belgium, Brussels, Belgium

[6] School of Atmosphere and Remote Sensing, Wuxi University, Wuxi, 214105, China

[7] Laboratoire d'Aérologie (LAERO), Université de Toulouse, CNRS, Toulouse, France

* Corresponding authors: David.Tarasick@ec.gc.ca and janejj.liu@utoronto.ca

Abstract: The vertical distribution of tropospheric O_3 from ozonesondes is compared with that from In-service Aircraft for a Global Observing System (IAGOS) measurements at 23 pairs of sites between about 30°S and 55°N, from 1995 to 2021. Profiles of tropospheric O_3 from IAGOS aircraft are in generally good agreement with ozonesonde observations, for Electrochemical concentration cells (ECC), Brewer-Mast, and Carbon-Iodine sensors, with average biases of 2.58 ppb, -0.28 ppb, and 0.67 ppb, and correlation coefficients (R) of 0.72, 0.82, and 0.66, respectively. Agreement between the aircraft and Indian-sonde observations is poor, with an average bias of 15.32 ppb and R of 0.44. The O_3 concentration observed by ECC sondes is on average higher by 5-10% than that observed by IAGOS aircraft, and the relative bias increases modestly with altitude. For other sonde types, there are some seasonal and altitude variations in the relative bias with respect to IAGOS measurements, but these appear to be caused by local differences. The distance between station and airport within 4° has little effect on the comparison results. For the ECC ozonesonde, the overall bias with respect to IAGOS measurements varies from 5.7 to 9.8 ppb, when the station pairs are grouped by station-airport distances of <1° (latitude and longitude), 1-2°, and 2-4°. Correlations for

these groups are R = 0.8, 0.9 and 0.7. These comparison results provide important information for merging ozonesonde and IAGOS measurement datasets. They can also be used to evaluate the relative biases of the different sonde types in the troposphere, using the aircraft as a transfer standard.

Key words: WOUDC; IAGOS; tropospheric O_3; vertical distribution; ozonesonde; aircraft

1 Introduction

Ozone (O_3) is a trace gas with small concentrations in the atmosphere (Ramanathan et al., 1985). It is an important greenhouse gas in the upper troposphere. In the planetary boundary layer, it is a major air pollutant (Lefohn et al., 2018; Monks et al., 2015). It can endanger human health, damage ecosystems, and affect climate change (Fu and Tai, 2015; Lefohn et al., 2018; Percy et al., 2003). Therefore, it is of importance to study the temporal and spatial variations in tropospheric O_3 including near-surface O_3 and mechanisms affecting the variations (Logan, 1985; Ma et al., 2020; Sharma et al., 2017; Young et al., 2018).

A large number of studies have been carried out on the spatiotemporal distribution, formation mechanisms, and transport characteristics of tropospheric O_3 (Li et al., 2020, 2021; Vingarzan, 2004; Wang et al., 2017, 2023; Xu et al., 2021; Yu et al., 2021). However, due to the limitation of observations, there are many unknowns on tropospheric O_3, especially the vertical distribution of tropospheric O_3. Satellites provide an effective platform for measuring O_3 globally. Satellite O_3 instruments, including TES, GOME, GOME-2, SCIAMACHY, OMI, and TROPOMI, have been in operation for decades (David et al., 2013; Ebojie et al., 2016; Hegarty et al., 2009; Hoogen et al., 1999; Hubert et al., 2021; Miles et al., 2015). Although satellite observations can provide detailed temporally- and horizontally-resolved maps of tropospheric O_3 columns, in general satellite data lack vertical resolution. While tropospheric differential absorption lidar can also provide vertical distribution information for tropospheric O_3 (Keckhut et al., 2004; Yang et al., 2023), there are very few routinely operating stations.

The principal sources of vertically-resolved, trend-quality observations of tropospheric O_3 are therefore balloon-borne ozonesondes, and IAGOS aircraft observations. The World Ozone and Ultraviolet Radiation Data Centre (WOUDC) and the In-service Aircraft for a Global Observing System database (IAGOS) house the data from these two observation programs with the longest

duration and the most global stations, which are the most widely used for tropospheric O_3 studies (Gaudel et al., 2020; Liao et al., 2021; Tarasick et al., 2019; Wang et al., 2022; Zang et al., 2024). These two datasets are used to study the distribution, variability and trends of tropospheric O_3, and its sources and transport, as well as satellite and model validation (Hu et al., 2017; Gaudel et al., 2018; 2020; Wang et al., 2022; Zhang et al., 2008). The first phase of the Tropospheric Ozone Assessment Report (TOAR-I), initiated in 2014, utilized available surface, ozonesonde, aircraft, and satellite observations to assess tropospheric O_3 trends from 1970 to 2014 (Schultz et al., 2017). Hu et al. (2017) found that the largest bias in a chemical transport model, GEOS-Chem, with respect to ozonesondes and IAGOS observations, is in high northern latitudes in winter-spring, where the simulated O_3 is 10-20 ppb lower. Wang et al. (2022) examined observed tropospheric O_3 trends, their attributions, and radiative impacts from 1995 to 2017, using aircraft observations from IAGOS, ozonesondes, and a multi-decadal GEOS-Chem chemical model simulation, and found increases in tropospheric O_3 (950-250 hPa) of 2.7 ± 1.7 ppbv per decade from IAGOS observations in the Northern Hemisphere and at 19 of 27 global ozonesonde sites averaging 1.9 ± 1.7 ppbv per decade. There are also a number of comparative studies on these two datasets (Zbinden et al., 2013; Staufer et al., 2013, 2014; Tanimoto et al., 2015; Tarasick et al., 2019). Staufer et al. (2013, 2014) used trajectory calculations to match air parcels sampled by both sondes and aircraft. Zbinden et al. (2013) compared coincidences (±24 hours) at three site pairs, while Tanimoto et al. (2015) examined simultaneous observations (±3 hours for sonde versus aircraft) at several site pairs less than 100 km apart. In general, these studies show small (6% or less) negative biases of aircraft measurements against ECC sondes. Tarasick et al. (2019) compared trajectory-mapped averages over 20°-70° N of ozonesonde and MOZAIC/IAGOS profiles and concluded that over 1994-2012 ozonesonde measurements were about 5 ± 1% higher in the lower troposphere and 8 ± 1% higher in the upper troposphere.

As shown above, the global O_3 vertical distribution datasets observed by WOUDC and IAGOS have been widely used in various studies. Still, a long-term and multi-site systematic comparison of these two datasets is rare, especially for the observations in the past three decades. In this study, we attempt to make the most comprehensive evaluation to date of the relative biases of IAGOS and sonde profiles, using as many station pairs as possible. We identify 23 suitable pairs of sites in the

WOUDC and IAGOS datasets from 1995 to 2021, compare the average vertical distribution of tropospheric O_3 shown by ozonesonde and aircraft measurements, and analyze their differences by ozonesonde type and by station-airport distance.

2 Data and methods

2.1 MOZAIC-IAGOS observations

The MOZAIC (Measurements of OZone and water vapor on Airbus In-service airCraft) program, initiated in 1994 and incorporated into the IAGOS (In-service Aircraft for a Global Observing System; www.iagos.org) program since 2011, takes advantage of commercial aircraft to provide worldwide in-situ measurements of several trace gases (e.g., O_3 and CO) and meteorological variables (e.g., water vapor) throughout the troposphere and the lower stratosphere (Marenco et al., 1998; Petzold et al., 2015; Nédélec et al., 2015). O_3 measurements are performed using a dual-beam UV-absorption monitor (time resolution of 4 seconds) with an instrumental uncertainty of ±2 ppbv+2% (Thouret et al., 1998; Blot et al., 2021). It should be noted that this is only the instrumental uncertainty, and does not include sampling uncertainties (possible losses) caused by the inlet line and the compressor before the UV-photometric measurements are made. Loss of O_3 on the inlet pump was an issue in earlier aircraft O_3 sampling programs (Brunner et al., 2001; Dias-Lalcaca et al., 1998; Schnadt Poberaj et al., 2007; Thouret et al., 2022), but Thouret et al. (1998) found it negligible for MOZAIC/IAGOS.

More details on the new IAGOS instrumentation can be found in Nédélec et al. (2015). The continuity of the dataset between the MOZAIC and IAGOS programs has been demonstrated based on their 2-year overlap (2011-2012) (Nédélec et al., 2015). Blot et al. (2021) evaluated the internal consistency of the O_3 measurements since 1994, which confirmed the instrumental uncertainty of ±2 ppb. Moreover, they found no bias drift amongst the different instrument units (six O_3 IAGOS-MOZAIC instruments, nine IAGOS-Core Package1 and the two instruments used in the IAGOS-CARIBIC aircraft).

2.2 WOUDC ozonesonde observations

The World Ozone and Ultraviolet Radiation Data Centre (WOUDC) is part of the Global Atmosphere Watch (GAW) program of the World Meteorological Organization

(https://woudc.org/data/explore.php). The WOUDC is operated by Environment and Climate Change Canada. WOUDC ozonesonde data have been evaluated in a number of WMO-sponsored international field intercomparisons (Attmannspacher and Dütsch, 1970, 1981; Kerr et al, 1994) and more recently in laboratory simulation chamber experiments using a standard reference photometer (Smit et al., 2007, 2024; Thompson et al., 2019). In the global ozonesonde network, while different ozonesonde types were common in the past, more than 95% of current sounding stations use electrochemical concentration cells (ECC). ECC ozonesondes have a precision of 3-5% (1-σ) while the precision of other sonde types is somewhat poorer, at about 5–10% for Brewer-Mast and the Japanese KC (Carbon-Iodine) sonde, and somewhat larger for the Indian-sonde (Kerr et al., 1994; Smit et al., 2007). Biases with respect to UV reference spectrometers have been estimated for ECC sondes at 1-5% in the troposphere (Smit et al., 2021; Tarasick et al., 2019, 2021).

2.3 Data processing

The two datasets were first screened for airport-sonde station pairs within a latitude separation of <4° and a longitude separation of <4°. Many sonde stations have observational records that do not overlap with the IAGOS period (1994-present). In addition, the IAGOS dataset has large gaps at many airports, because the frequency of visits to airports by aircraft that take part in IAGOS depends on commercial airlines' operating constraints. In total, 23 station pairs (Fig. 1) were identified with a separation of less than 4° in both latitude and longitude, and coincident observations over at least nine months. The majority of the 23 ozonesonde site records are ECC (17), while four are Indian-sonde, one Brewer-Mast, and one Carbon-Iodine (the Japanese KC sonde). These stations were divided into 3 groups according to the distance (D) between the ozonesonde station and the airport: D<1°, 1°<D<2°, and 2°<D<4°. Specific information on the comparison stations is shown in Table 1.

The observation times of the ozonesonde and aircraft are generally not the same. Ozonesondes are typically launched once a week, although a few stations have more frequent launches. The aircraft records generally contain more frequent observations, but observation times vary. For the selected 23 stations, we calculated the mean O_3 vertical profiles at 1km resolution (the first layer is from the surface to 1 km above sea level) for each month during the observational period for the two datasets. A minimum of four aircraft profiles were required to estimate a monthly mean profile; because

ozonesonde launches are typically only a few times per month, no minimum was required to estimate a monthly mean profile. Only data with monthly means in both datasets were included for further analysis. Comparisons between the two datasets were made by ozonesonde type and by station-airport distance.

3. Results and discussion

3.1 Comparison of the vertical profiles of tropospheric O_3 from four types of ozonesondes and aircraft observations

Previous intercomparisons of sondes launched on the same balloon (Attmannspacher and Dütsch, 1970, 1981; Beekmann et al, 1994, 1995; Deshler et al., 2008; Hilsenrath et al., 1986; Kerr et al, 1994; Smit et al., 2007) have shown that sondes of different types respond somewhat differently to the same O_3 vertical profile; that is, they have relative biases, that vary with altitude. Fig. 2 therefore compares the mean vertical profiles of tropospheric O_3 from ozonesonde and aircraft measurements, separated by ozonesonde type. Both O_3 concentrations and absolute differences between ozonesonde and aircraft increase with altitude, especially above 9 km. Average tropospheric O_3 profiles observed by ECC, Brewer-Mast, and Carbon-Iodine sondes are in good agreement with aircraft measurements, with biases of 2.58 ppb, -0.28 ppb and 0.67 ppb, while the agreement with the Indian-sonde is poorer, with a bias of 15.32 ppb. The Indian-sonde average also shows a linear increase with altitude, while the aircraft measurements indicate an O_3 decrease with altitude above 8 km (Fig. 2b). This behavior is most clearly related to the comparisons of stations 2°-4° apart in spring (Fig. S9).

These results are broadly consistent with those from JOSIE 1996 (Smit et al. 1996; Smit and Kley, 1998; Thompson et al., 2019), and with the northern hemisphere average result from Tarasick et al. (2019). (Their Figure 20b; note that it is largely based on ECC sondes, and the scale is inverted (IAGOS-sondes) from the sense we use here.)

Fig. 3 shows correlation plots of monthly mean O_3 at 1 km vertical intervals for months when both IAGOS and ozonesonde data are available at the same location. While these monthly averages are of data not necessarily coincident in time, Fig. 3 indicates that the data compare well on this timescale, with correlation coefficients (R) of 0.71, 0.88 and 0.66, respectively (Fig. 3a-3c). The

agreement between the Indian-sonde and aircraft observations is poor, however, with an R of only 0.44 (Fig. 3d). The RMSE of O_3 observed with the four types of ozonesondes (ECC, Brewer-Mast, Carbon-Iodine and Indian-sonde) and the aircraft is 15.99 ppb, 14.15 ppb, 16.26 ppb and 29.85 ppb, respectively. After calculation, we obtained the slopes and offsets of ECC, Brewer-mast, Carbon-iodine and Indian-sonde without forcing the fitted lines through zero, the slope is 0.71, 0.88, 0.56 and 0.74, respectively, and the offset is 18.94 ppb, 6.89ppb, 27.48ppb and 27.84ppb. When we force the intercept to zero for the regressions, the slope is larger than the slope without forcing the fitted lines through zero (fig. 3). In generally, when O_3 is zero both the ozonesondes and the aircraft will measure zero. However, there is an offset in the fit of the two data sets due to potential causes for systematic differences during the observation measurement process, e.g., high background current in the sonde data.

Fig**.** 2 shows that the mean differences between ozonesonde and aircraft measurements vary significantly with altitude. This can also be observed clearly from the relative differences (RD), expressed as $(O_{3\text{-ozonesonde}} - O_{3\text{-aircraft}})/ O_{3\text{-aircraft}} \times 100\%$ (Fig. 4). O_3 concentrations from ECC measurements are higher than those from aircraft measurements in all altitudes except at the surface. Mean O_3 concentrations reported by Brewer-Mast sondes are lower than those from IAGOS below 7 km, but higher between 7 and 12 km. O_3 concentrations reported by Carbon-Iodine sondes are higher than those observed from aircrafts below 2 km, but significantly lower above 8 km. In relative terms, the bias between ECC sonde and aircraft measurements varies little with altitude, except near the ground. The mean relative bias for Brewer-Mast measurements is at an absolute maximum of -19 % near the ground, but increases slowly above 3 km, and is positive above 7 km, reaching more than +10 % at 10-11 km. The relative bias for Carbon-Iodine measurements is about 8% below 2 km, becomes quite small from 2 - 8 km, and becomes large and negative above 8 km.

The Indian-sonde observations show much larger mean differences from the aircraft measurements. Biases are everywhere positive, and as high as nearly 60% or 30 ppb, with much higher uncertainty (standard errors) at each altitude as well (Fig. 2b, Fig. 4).

The region below 3 km has many local ozone sources and sinks (cities, airports, rural environment, etc). In comparison, the region above 8 km is significantly influenced by stratosphere-troposphere exchange, jet streams, and tropopause folds. Fig. S1 shows that the R between ozonesondes and

aircraft observations is higher near the ground (< 2 km) and at high altitudes (> 10 km). This shows that although the influencing factors of O_3 near the ground and at high altitudes are more complex, their long-term temporal variation characteristics are similar. The influences of cities, airports, rural environment, stratosphere-troposphere exchange, jet streams, tropopause folds, etc., have a more significant impact on the concentration of O_3 in the short term.

The correlation between four types of ozonesondes and aircraft observations also varies with altitude (Fig. S1). From 0-8 km, the correlation between ECC and aircraft observations decreases with altitude, with R being 0.71 at 0-1 km and reaching a minimum of 0.29 at 8-9 km; from 8-12 km, R increases with altitude, reaching 0.49 at 11-12 km. The correlation between the other three ozonesondes (Brewer-mast, Indian-sonde and Carbon-iodine) and the aircraft observations all vary with altitude, with different inflection points. The number of stations for these three types of ozonesondes is small (Table 1). Therefore, local variable influences on O_3 are more important, so R varies more with altitude.

The bias and RMSE with respect to the aircraft observations of the four types of ozonesondes at 8-12 km are higher than that at other altitudes. In contrast, the bias and RMSE values below 8 km are smaller and vary less with altitude, consistent with the vertical distribution characteristics of O_3 concentration in Fig. 2. This is likely due to the higher concentration of O_3 and the typically larger difference in spatial distance between ozonesonde and aircraft observations at 8-12km.

In addition, the bias and RMSE relative to the aircraft observations at different altitudes for ECC, Carbon-iodine and Brewer-mast sondes are lower than those for the Indian-sonde, which is similar to the results of the above analysis of O_3 concentration.

It should be noted that these comparisons only give an average relative bias between sondes and IAGOS. The true value of the ozone profile remains unknown, as do the absolute biases of sondes and IAGOS.

3.2 Seasonal variations in relative biases between ozonesondes and IAGOS

Fig. 5 compares mean profiles observed by ECC ozonesondes and IAGOS, separated by season. There are modest seasonal differences in the relative bias profiles, with somewhat larger average biases in winter and spring, but average biases are all positive (ECC sondes higher) and at all levels

233 the average seasonal biases are not statistically different.

234 The modest seasonal differences that are apparent in Fig. 5 and in Figs. S2-S4 are likely due to the
235 modest sample size (for ECC sondes) and small sample sizes (for other types). The actual
236 coincidence in time for profiles can range from less than one day to about 1-3 weeks, depending on
237 the number of ozonesonde and aircraft O_3 profiles collected within each month-bin. This means the
238 larger the atmospheric variability of O_3 is, the larger the real differences between ozonesonde and
239 aircraft O_3 can become, particularly when the number of profiles within a month-bin are small. In
240 addition, there are errors due to variations in the aircraft take-off and landing trajectories and the
241 balloon rise rate, the geographical location of the observation stations (and any associated
242 meteorological differences) and any systematic difference in standard observational times.

243 Table 2 indicates that in all four seasons ECC data correlate well with aircraft observations, with R
244 ranging from 0.71 to 0.76, but with larger average biases in winter and spring, as noted. It is not
245 clear if these seasonal average differences in bias are significant, as the uncertainty ranges on the
246 seasonal averages (lower plot of Fig. 5) overlap.

247 The vertical distribution of tropospheric O_3 observed by Brewer-Mast and IAGOS aircraft in the
248 four seasons is similar (Fig. S2). Differences are also similar, except above 7 km, where the
249 uncertainties are larger, and in general the uncertainty ranges on the seasonal difference averages
250 overlap. Since these comparisons come from only one station pair, some of the differences may be
251 attributable to local differences in topography and meteorology. Table 2 shows that correlations for
252 the ensemble of Brewer-Mast stations are higher than those for ECC stations. Like the ECC sondes,
253 average biases are all positive, but this is determined by the biases above 7 km (Fig. 4); unlike the
254 ECCs, biases are negative in the lowest 3 km.

255 The vertical distribution of tropospheric O_3 concentrations observed by Carbon-Iodine sondes and
256 IAGOS aircraft in the four seasons are similar, except in summer when the tropopause is high (Fig.
257 S3). The difference plots are fairly similar, except in the lowest 3 km, where differences become
258 quite large in summer. Like the previous comparison for Brewer-Mast sondes, these comparisons
259 come from only one station pair, and so the large differences in the boundary layer in summer are
260 likely due to local O_3 production sampled by the sonde but not the aircraft. Likely for this reason,
261 the consistency between Carbon-Iodine and aircraft observations is poor in summer, with R being

only 0.46 (Table 2). For the other three seasons it is fairly good.

The tropospheric O_3 observed by Indian-sondes displays a consistently high bias relative to IAGOS in all seasons, and the seasonal difference plots are quite similar, except in the lowest 3 km in winter (Fig. S4). This different behavior in winter is likely due to local ozone production sampled by the aircraft but not the sonde. Temperature inversions are common in the winter in northern India and trap local pollution. The very low values registered by the aircraft near the surface in summer also suggest local effects, in this case titration by NO_x.

The tropospheric O_3 observed by Indian-sonde in the four seasons is 43.3-79.4 ppb, 31.4-80.2 ppb, 42.2-69.6 ppb and 51.5-87.5 ppb, and that observed by aircraft in the four seasons is 22.8-60.1 ppb, 14.8-47.1 ppb, 25.0-44.1 ppb and 35.6-53.3 ppb (Fig. S4). The tropospheric O_3 observed in Indian-sonde in the four seasons increases with height almost linearly. The tropospheric O_3 observed by aircraft first increases and then decreases with altitude in spring, summer and autumn, while in winter, it first decreases and then increases with altitude. The tropospheric O_3 observed by the Indian-sonde and the aircraft is quite different, and the RD in the four seasons is 6.3% to 47.5%, 22.6% to 52.9%, 26.4% to 40.6% and 5.13% to 39.13%. Table 2 indicates poor consistency between Indian-sonde and aircraft observations in all four seasons, with R in winter only 0.18. The bias and RMSE in winter are the largest, at 40.07 ppb and 64.99 ppb. The bias, R and RMSE in the other three seasons are smaller, and the differences between them slight.

3.3 Dependence of relative biases on station-airport distances

A major concern with comparing IAGOS and ozonesonde observations is that the stations and airports are not generally co-located, and even where they are close, the flight paths taken by balloon and aircraft are quite different. Fig. 6 compares the average vertical distribution of tropospheric O_3 observed at different station-airport distances by ECC sondes and IAGOS aircraft. Note that we continue to separate sonde station data by type --- only ECC data are used here. Sonde-aircraft pairs have been grouped by station-airport distance (Table 1). The differences in average bias vary only very modestly between the different station-airport distance categories, and those differences are not statistically different at the 95% confidence level (Fig. 6d). This, partially owing presumably to the use of mean monthly averages, is encouraging, as this provides further evidence that the average bias we have derived is an artifact strictly of instrument differences.

Table 3 indicates that the bias variation between ECC and aircraft observations at different station-airport distances is small, ranging from 5.7 ppb to 9.8 ppb. Correlations for these groupings are also fairly similar, at R = 0.8, 0.9 and 0.7.

Compared with ECC sondes, the consistency between the Indian-sonde and aircraft observations is poor at all station-airport distances, with much larger biases, and poor correlations, with R = 0.2 to 0.4. Nevertheless, Fig. S5 shows that the profiles of average differences are quite similar for station-airport distances < 1°, and distances of 2°-4° (Fig. S5c).

Fig. 7 and Figs. S6-S8 examine possible seasonal variation in the differences at different station-airport distances, for ECC sondes. The mean differences for the different station-airport distance categories are larger than for the annual averages (Fig. 6), but in general those differences are not statistically different at the 95% confidence level (Figs. 7d and S6d-S8d).

3.4 Comparison of ozonesonde relative biases under operational conditions using IAGOS observations as a transfer standard

The foregoing discussion demonstrates that, consistent with previous work, there is a fairly constant relative bias between IAGOS and sondes, with considerable dependence on sonde type, as expected from previous sonde intercomparisons like JOSIE 1996. Although uncertainties are sizeable due to the relatively sparse nature of the available data, we find consistent differences at all sites, with little dependence on season or on station-airport separation, and little regional dependence (not shown). Notwithstanding this overall sonde-IAGOS bias, we can use these station-airport comparisons to derive relative biases of the different sonde types in use in the global network.

This does not assume that the aircraft data are unbiased. The true value of the O_3 profile (or even its average) remains unknown, as do the absolute biases of sondes and IAGOS. It does assume:

1. That the measurement errors are random and normally distributed;
2. That there is one, constant bias for each measurement type (that is, if, for example, the Indian sonde has changed over the period of comparison, or the IAGOS instruments have different biases, there would be additional error that is not included in our uncertainty estimate);
3. That the measurement biases are not dependent on the geographic location or other variability of the O_3 profile. This does not assume that the average O_3 profile is the same, just that the instruments

respond in the same way.

With these assumptions we can use the results of Fig. 2 to estimate the relative biases of each sonde type to each other. The uncertainty of the comparisons will be the quadratic sum of the uncertainties of the two IAGOS-sonde comparisons. The results are shown in Table 4. This intercomparison of the different sonde types has an important advantage: it compares ozonesonde relative biases under operational conditions, as it compares the data that are actually in databases like the WOUDC. It also fills a gap, as the last WMO international intercomparison involving all four sonde types was JOSIE 1996. These results are broadly consistent with those from JOSIE 1996 (Smit and Kley, 1998; their Table 8 and Fig. 11).

In fact, the types of ozonesonde have changed during long-term observations at some stations (e.g. Uccle and Payerne). De Backer et al. (1998) showed that with the use of an appropriate correction procedure, accounting for the loss of pump efficiency with decreasing pressure and temperature, it is possible to reduce the mean difference between O_3 profiles obtained with both types of sondes below 3%, which is statistically insignificant over nearly the whole operational altitude range (from the ground to 32 km). Stübi et al. (2008) also found that the O_3 difference between the Brewer-Mast and the ECC ozonesonde data shows good agreement between the two sonde types, and the profile of the O_3 difference is limited to ±5% (±0.3 mPa) from the ground to 32 km. The results for Brewer-Mast sondes in Table 4 should also be applicable to the older Payerne and Uccle records, and are generally consistent with these results and with those for the older Canadian records (Tarasick et al., 2002; 2016).

The results in Table 4 will be quite valuable for addressing the problem of relative biases when merging ozonesonde data into global climatologies (e.g. McPeters et al., 2007; McPeters and Labow, 2012; Bodeker et al., 2013; Liu et al., 2013; Hassler et al., 2018;).

4 Conclusions

The vertical distribution of tropospheric O_3 observed by ozonesondes and IAGOS aircraft sensors are compared at 23 pairs of sites between about 30°S and 55°N from 1995 to 2021. Overall, ECC, Brewer-Mast, and Carbon-Iodine sondes agree reasonably well with aircraft observations, with average biases of 2.58 ppb, -0.28 ppb, and 0.67 ppb, and correlation coefficients of 0.72, 0.82, and 0.66, respectively. The agreement between the aircraft and Indian-sonde observations is poor, with

an average bias of 15.32 ppb and R of 0.44. Ozonesondes and aircraft observations have smaller R in the middle troposphere, but larger bias and RMSE in the upper troposphere. The bias and RMSE relative to the aircraft observations at different altitudes for ECC, Carbon-iodine and Brewer-mast sondes are lower than those for the Indian-sonde.

Notwithstanding this general agreement, all sonde types show significant average biases with respect to IAGOS. The O_3 concentration observed by ECC sondes is on average higher by 5-10% than that observed by IAGOS aircraft, and the relative bias increases modestly with altitude. Seasonal variations in the relative bias are not in general statistically significant. The distance between station and airport within 4° also has little effect on the comparison results. When the ECC station pairs are grouped by station-airport distances of <1° (latitude and longitude), 1-2°, and 2-4°, biases with respect to IAGOS measurements vary from 5.7 to 9.8 ppb, and correlations from 0.7 to 0.9.

Thus, the observed average relative bias between sondes and IAGOS found in this study, also noted by previous authors (Zbinden et al., 2013; Staufer et al., 2013, 2014; Tanimoto et al., 2015; Tarasick et al., 2019), is a robust result. Possible reasons for the difference include: side reactions that cause sondes to produce excess iodine (Saltzman and Gilbert, 1959), and/or loss of O_3 on the inlet pump that could cause IAGOS monitors to read low at pressures below 800 hPa. The latter was an issue in earlier aircraft O_3 sampling programs (Schnadt Poberaj et al., 2007; Dias-Lalcaca et al., 1998; Brunner et al., 2001), but Thouret et al. (1998) found it negligible for MOZAIC/IAGOS. A recent intercomparison campaign at the World Calibration Centre for Ozone Sondes (WCCOS) in Julich in June 2023 indicates that the pumps do not greatly influence the ozone IAGOS measurements between 1000 and 200 hPa. The IAGOS-CORE O_3 measurements (Package 1 with pressurization pumps) and IAGOS-CARIBIC O_3 measurements differ by less than 2%, and the WCCOS reference UV photometer measurements are usually higher by 1-2% (to a maximum of 5%) compared to both IAGOS instruments (Blot et al., 2021; Nédélec et al., 2015; Thouret et al., 2022). IAGOS-CARIBIC does not have pressurization system, so that's why the good comparison between both IAGOS systems means a lot.

However, as noted by Saltzman and Gilbert (1959), the differences in stoichiometry found at different pH values imply that the chemistry of reaction of O_3 with KI is complex, involving

reactions that cause loss of iodine, as well as reactions other than the principal one that produce additional iodine. Several authors have noted the existence of slow side reactions involving the phosphate buffer, with a time constant of about 20 minutes, that may also increase the stoichiometry from 1.0 (Tarasick et al., 2021, Smit et al., 2024). Furthermore, evaporation causes the concentration of the sensing solution to increase, which can further enhance the stoichiometry, by concentrating the phosphate buffer, and to a lesser degree, by increasing the concentration of the KI itself (Johnson et al., 2002). These factors could contribute to the observed average relative bias between sondes and IAGOS found in this study.

This result implies that care must be taken when merging ozonesonde and IAGOS measurement datasets. While the aircraft and sonde measurements are often complementary, filling in important spatial gaps that would otherwise exist if only one type were used, the records are not typically over the same period, and so merging can introduce spurious jumps if relative biases are not taken into account.

The importance of O_3 in the troposphere as an air pollutant and a greenhouse gas, and therefore of accurate measurements of its temporal and spatial distribution implies that it will be important to resolve the causes of this bias, and so further research involving more direct comparisons of IAGOS instrumentation and ozonesondes, e.g. in the WCCOS chamber, are strongly recommended.

These results are also useful to evaluate the relative biases of the different sonde types in the troposphere, using the aircraft as a transfer standard. This intercomparison of the different sonde types has the advantage that it compares ozonesonde relative biases under operational conditions; that is, the data that are actually in databases like the WOUDC. These results will be invaluable for addressing relative biases when merging ozonesonde data into global climatologies (e.g. Bodeker et al., 2013; Hassler et al., 2018; Liu et al., 2013; McPeters et al., 2007; McPeters and Labow, 2012).

Competing interests. The contact authors have declared that none of the authors has any competing interests.

Data availability. The global ozone sounding data were acquired from the World Ozone and Ultraviolet Radiation Data Center (http://www.woudc.org) operated by Environment Canada. The IAGOS data are created with support from the European Commission, national agencies in Germany

(BMBF), France (MESR), and the UK (NERC), and the IAGOS member institutions (http://www.iagos.org/partners).

Author contributions. **HW**: Data curation, Methodology, Validation, Visualization, Writing - original draft preparation, Writing - review & editing, Funding acquisition. **LS**: Methodology, Investigation, Writing - original draft. **DWT**: Data curation, Resources, Conceptualization, Supervision, Writing - original draft preparation, Writing - review & editing. **JL**: Data curation, Resources, Methodology, Conceptualization, Supervision, Writing - original draft preparation, Writing - review & editing, Funding acquisition. **TZ**: Funding acquisition, Writing - review & editing. **HGJS** and **RVM**: Writing - review & editing. **HGJS** and **RB**: Acquisition of IAGOS data, Quality assessment IAGOS data.

Acknowledgments. We thank many whose dedication makes datasets used in this study possible. The global O_3 sounding data were acquired from the World Ozone and Ultraviolet Radiation Data Center (http://www.woudc.org) operated by Environment Canada, Toronto, Canada, under the auspices of the World Meteorological Organization. Flight-based atmospheric chemical measurements are from IAGOS. IAGOS is funded by the European Union projects IAGOS-DS and IAGOS-ERI. The IAGOS data are created with support from the European Commission, national agencies in Germany (BMBF), France (MESR), and the UK (NERC), and the IAGOS member institutions (http://www.iagos.org/partners). The participating airlines (Lufthansa, Air France, Austrian, China Airlines, Iberia, Cathay Pacific, Air Namibia, Sabena) supported IAGOS by carrying the measurement equipment free of charge since 1994. We are also thankful to the Digital Research Alliance of Canada at the University of Toronto for facilitating data analysis.

Financial support. This study was supported by the Natural Science and Engineering Council of Canada (Grant No. RGPIN-2020-05163), the National Key Research and Development Program of China (Grant No., 2022YFC3701204), the National Natural Science Foundation of China (42275196 and 41830965), the Natural Science Foundation of Jiangsu Province (BK20231300), and Wuxi University Research Start-up Fund for Introduced Talents (2023r035).

436 **References**

437 Attmannspacher, A., and Dütsch,, H.U., 1970. International ozone sonde intercomparison at the
438 Observatory Hohenpeissenberg, Ber. Dtsch. Wetterdienstes, 120, 1-85.

439 Attmannspacher, A., and Dütsch, H.U., 1981. Second international ozone sonde intercomparison at
440 the Observatory Hohenpeissenberg, Ber. Dtsch. Wetterdienstes, 157, 1-64.

441 Beekmann, M., Ancellet, G., Megie, G., Smit, H.G.J., Kley, D., 1994. Intercomparison campaign of
442 vertical ozone profiles including electrochemical sondes of ECC and Brewer-Mast type and a
443 ground based UV-differential absorption lidar. Journal of Atmospheric Chemistry, 19, 259-288.
444 19.

445 Beekmann, M., Ancellet, G., Martin, D., Abonnel, C., Duverneuil, G., Eideliman, F., Bessemoulin,
446 P., Fritz, N., Gizard, E., 1995. Intercomparison of tropospheric ozone profiles obtained by
447 electrochemical sondes, a ground based lidar and an airborne UV-photometer. Atmospheric
448 Environment, 29(9), 1027-1042.

449 Bernhard, G.H., Bais, A.F., Aucamp, P.J., Klekociuk, A.R., Liley, J.B., McKenzie, R.L., 2023.
450 Stratospheric ozone, UV radiation, and climate interactions. Photochemical and
451 Photobiological Sciences, 1-53.

452 Blot, R., Nedelec, P., Boulanger, D., Wolff, P., Sauvage, B., Cousin, J.-M., Athier, G., Zahn, A.,
453 Obersteiner, F., Scharffe, D., Petetin, H., Bennouna, Y., Clark, H., Thouret, V., 2021. Internal
454 consistency of the IAGOS ozone and carbon monoxide measurements for the last 25 years.
455 Atmospheric Measurement Techniques, 14, 3935-3951, https://doi.org/10.5194/amt-14-3935-
456 2021.

457 Bodeker, G. E., Hassler, B., Young, P. J., Portmann, R. W., 2013. A vertically resolved, global, gap-
458 free ozone database for assessing or constraining global climate model simulations. Earth
459 System Science Data, 5, 31-43, https://doi.org/10.5194/essd-5-31-2013.

460 Brunner, D., J. Staehelin, D. Jeker, H., Wernli, U. Schumann, 2001. Nitrogen oxides and ozone in
461 the tropopause region of the Northern Hemisphere: Measurements from commercial aircraft in
462 1995/96 and 1997. Journal of Geophysical Research: Atmospheres, 106, 27673-27699.

463 Callis, L.B., Boughner, R.E., Natarajan, M., Lambeth, J.D., Baker, D.N., Blake, J.B., 1991. Ozone
464 depletion in the high latitude lower stratosphere: 1979-1990. Journal of Geophysical Research:

Atmospheres, 96(D2), 2921-2937.

David, L.M. and Nair, P.R., 2013. Tropospheric column O_3 and NO_2 over the Indian region observed by Ozone Monitoring Instrument (OMI): Seasonal changes and long-term trends. Atmospheric Environment, 65, 25-39.

De Backer, H., De Muer, D., De Sadelaer, G., 1998. Comparison of ozone profiles obtained with Brewer-Mast and Z-ECC sensors during simultaneous ascents. Journal of Geophysical Research: Atmospheres, 103(D16), 19641-19648.

Deshler, T., Mercer, J.L., Smit, H.G., Stubi, R., Levrat, G., Johnson, B.J., Oltmans, S.J., Kivi, R., Thompson, A.M., Witte, J., Davies, J., 2008. Atmospheric comparison of electrochemical cell ozonesondes from different manufacturers, and with different cathode solution strengths: The Balloon Experiment on Standards for Ozonesondes. Journal of Geophysical Research: Atmospheres, 113(D4), D04307, doi:10.1029/2007JD008975.

Dias-Lalcaca, P., Brunner, D., Imfeld, W., Moser, W., Staehelin, J., 1998. An automated system for the measurement of nitrogen oxides and ozone concentrations from a passenger aircraft: Instrumentation and first results of the NOXAR project. Environmental Science and Technology, 32(20), 3228-3236.

Ebojie, F., Burrows, J.P., Gebhardt, C., Ladstätter-Weißenmayer, A., Von Savigny, C., Rozanov, A., Weber, M., Bovensmann, H., 2016. Global tropospheric ozone variations from 2003 to 2011 as seen by SCIAMACHY. Atmospheric Chemistry and Physics, 16(2), 417-436.

Fu, Y. and Tai, A.P.K., 2015. Impact of climate and land cover changes on tropospheric ozone air quality and public health in East Asia between 1980 and 2010. Atmospheric Chemistry and Physics, 15(17), 10093-10106.

García, O.E., Sanromá, E., Schneider, M., Hase, F., León-Luis, S.F., Blumenstock, T., Sepúlveda, E., Redondas, A., Carreño, V., Torres, C., Prats, N., 2022. Improved ozone monitoring by ground-based FTIR spectrometry. Atmospheric Measurement Techniques, 15(8), 2557-2577.

García, O.E., Schneider, M., Sepúlveda, E., Hase, F., Blumenstock, T., Cuevas, E., Ramos, R., Gross, J., Barthlott, S., Röhling, A.N., Sanromá, E., 2021. Twenty years of ground-based NDACC FTIR spectrometry at Izaña Observatory-overview and long-term comparison to other techniques. Atmospheric Chemistry and Physics, 21(20), 15519-15554.

Gaudel, A., Cooper, O.R., Ancellet, G., Barret, B., Boynard, A., Burrows, J.P., Clerbaux, C., Coheur, P.F., Cuesta, J., Cuevas, E., Doniki, S., 2018. Tropospheric Ozone Assessment Report: Present-day distribution and trends of tropospheric ozone relevant to climate and global atmospheric chemistry model evaluation. Elementa: Science of the Anthropocene, 6.

Gaudel, A., Cooper, O.R., Chang, K.L., Bourgeois, I., Ziemke, J.R., Strode, S.A., Oman, L.D., Sellitto, P., Nédélec, P., Blot, R., Thouret, V., 2020. Aircraft observations since the 1990s reveal increases of tropospheric ozone at multiple locations across the Northern Hemisphere. Science Advances, 6(34), eaba8272.

Gebhardt, C., Rozanov, A., Hommel, R., Weber, M., Bovensmann, H., Burrows, J.P., Degenstein, D., Froidevaux, L., Thompson, A.M., 2014. Stratospheric ozone trends and variability as seen by SCIAMACHY from 2002 to 2012. Atmospheric Chemistry and Physics, 14(2), 831-846.

Hassler, B., Kremser, S., Bodeker, G. E., Lewis, J., Nesbit, K., Davis, S. M., Chipperfield, M. P., Dhomse, S. S., Dameris, M., 2018, An updated version of a gap-free monthly mean zonal mean ozone database. Earth System Science Data, 10, 1473-1490.

Hegarty, J., Mao, H., Talbot, R., 2009. Synoptic influences on springtime tropospheric O_3 and CO over the North American export region observed by TES. Atmospheric Chemistry and Physics, 9(11), 3755-3776.

Hilsenrath, E., Attmannspacher, W., Bass, A., Evans, W., Hagemeyer, R., Barnes, R., Komhyr, W., Mauersberger, K., Mentall, J., Proffitt, M., Robbins, D., 1986. Results from the balloon ozone intercomparison campaign (BOIC). Journal of Geophysical Research: Atmospheres, 91(D12), 13137-13152.

Hoogen, R., Rozanov, V.V., Burrows, J.P., 1999. Ozone profiles from GOME satellite data: Algorithm description and first validation. Journal of Geophysical Research: Atmospheres, 104(D7), 8263-8280.

Hu, L., Jacob, D.J., Liu, X., Zhang, Y., Zhang, L., Kim, P.S., Sulprizio, M.P., Yantosca, R.M., 2017. Global budget of tropospheric ozone: Evaluating recent model advances with satellite (OMI), aircraft (IAGOS), and ozonesonde observations. Atmospheric Environment, 167, 323-334.

Hubert, D., Heue, K.P., Lambert, J.C., Verhoelst, T., Allaart, M., Compernolle, S., Cullis, P.D., Dehn, A., Félix, C., Johnson, B.J., Keppens, A., 2021. TROPOMI tropospheric ozone column data:

geophysical assessment and comparison to ozonesondes, GOME-2B and OMI. Atmospheric Measurement Techniques, 14(12), 7405-7433.

Johnson, B.J., Oltmans, S.J., Vömel, H., Smit, H.G.J., Deshler, T., Kroeger, C., 2002. ECC Ozonesonde pump efficiency measurements and tests on the sensitivity to ozone of buffered and unbuffered ECC sensor cathode solutions. Journal of Geophysical Research: Atmospheres, 107(4393), 10-1029. doi: 10.1029/2001JD000557.

Keckhut, P., McDermid, S., Swart, D., McGee, T., Godin-Beekmann, S., Adriani, A., Barnes, J., Baray, J.L., Bencherif, H., Claude, H., di Sarra, A.G., 2004. Review of ozone and temperature lidar validations performed within the framework of the Network for the Detection of Stratospheric Change. Journal of Environmental Monitoring, 6(9), 721-733.

Kerr, J.B., Fast, H., McElroy, C.T., Oltmans, S.J., Lathrop, J.A., Kyro, E., Paukkunen, A., Claude, H., Köhler, U., Sreedharan, C.R., Takao, T., 1994. The 1991 WMO international ozonesonde intercomparison at Vanscoy, Canada. Atmosphere-Ocean, 32(4), 685-716.

Lefohn, A.S., Malley, C.S., Smith, L., Wells, B., Hazucha, M., Simon, H., Naik, V., Mills, G., Schultz, M.G., Paoletti, E., De Marco, A., 2018. Tropospheric ozone assessment report: Global ozone metrics for climate change, human health, and crop/ecosystem research. Elementa: Science of the Anthropocene, 6.

Li, K., Jacob, D.J., Liao, H., Qiu, Y., Shen, L., Zhai, S., Bates, K.H., Sulprizio, M.P., Song, S., Lu, X., Zhang, Q., 2021. Ozone pollution in the North China Plain spreading into the late-winter haze season. Proceedings of the National Academy of Sciences, 118(10), e2015797118.

Li, K., Jacob, D.J., Shen, L., Lu, X., De Smedt, I., Liao, H., 2020. Increases in surface ozone pollution in China from 2013 to 2019: anthropogenic and meteorological influences. Atmospheric Chemistry and Physics, 20(19), 11423-11433.

Liao, Z., Ling, Z., Gao, M., Sun, J., Zhao, W., Ma, P., Quan, J., Fan, S., 2021. Tropospheric ozone variability over Hong Kong based on recent 20 years (2000-2019) ozonesonde observation. Journal of Geophysical Research: Atmospheres, 126(3), e2020JD033054.

Liu, G., Liu, J., Tarasick, D.W., Fioletov, V.E., Jin, J.J., Moeini, O., Liu, X., Sioris, C.E., Osman, M., 2013. A global tropospheric ozone climatology from trajectory-mapped ozone soundings. Atmospheric Chemistry and Physics, 13(21), 10659-10675.

552 Logan, J.A., 1985. Tropospheric ozone: Seasonal behavior, trends, and anthropogenic
553 influence. Journal of Geophysical Research: Atmospheres, 90(D6), 10463-10482.
554 Ma, Y., Ma, B., Jiao, H., Zhang, Y., Xin, J., Yu, Z., 2020. An analysis of the effects of weather and
555 air pollution on tropospheric ozone using a generalized additive model in Western China:
556 Lanzhou, Gansu. Atmospheric Environment, 224, 117342.
557 McPeters, R.D., Labow, G.J., Logan, J.A., 2007. Ozone climatological profiles for satellite retrieval
558 algorithms. Journal of Geophysical Research: Atmospheres, 112(D5), D05308.
559 doi:10.1029/2005JD006823.
560 McPeters, R.D. and Labow, G.J., 2012. Climatology 2011: An MLS and sonde derived ozone
561 climatology for satellite retrieval algorithms. Journal of Geophysical Research: Atmospheres,
562 117(D10), D10303. doi:10.1029/2011JD017006.
563 Miles, G.M., Siddans, R., Kerridge, B.J., Latter, B.G., Richards, N.A.D., 2015. Tropospheric ozone
564 and ozone profiles retrieved from GOME-2 and their validation. Atmospheric Measurement
565 Techniques, 8(1), 385-398.
566 Meng, K., Zhao, T., Xu, X., Zhang, Z., Bai, Y., Hu, Y., Zhao, Y., Zhang, X., Xin, Y., 2022. Influence
567 of stratosphere-to-troposphere transport on summertime surface O_3 changes in North China
568 Plain in 2019. Atmospheric Research, 276, 106271.
569 Monks, P.S., Archibald, A.T., Colette, A., Cooper, O., Coyle, M., Derwent, R., Fowler, D., Granier,
570 C., Law, K.S., Mills, G.E., Stevenson, D.S., 2015. Tropospheric ozone and its precursors from
571 the urban to the global scale from air quality to short-lived climate forcer. Atmospheric
572 Chemistry and Physics, 15(15), 8889-8973.
573 Nédélec, P., Blot, R., Boulanger, D., Athier, G., Cousin, J.M., Gautron, B., Petzold, A., Volz-Thomas,
574 A., Thouret, V., 2015. Instrumentation on commercial aircraft for monitoring the atmospheric
575 composition on a global scale: the IAGOS system, technical overview of ozone and carbon
576 monoxide measurements. Tellus B: Chemical and Physical Meteorology, 67(1), 27791.
577 https://doi.org/10.3402/tellusb.v67.27791@zelb20.2016.68.issue-s1
578 Percy, K.E., Legge, A.H., Krupa, S.V., 2003. Tropospheric ozone: a continuing threat to global
579 forests? Developments in Environmental Science, 3, 85-118.
580 Perlwitz, J., Pawson, S., Fogt, R.L., Nielsen, J.E., Neff, W.D., 2008. Impact of stratospheric ozone

hole recovery on Antarctic climate. Geophysical Research Letters, 35(8). https://doi.org/10.1029/2008GL033317.

Ramanathan, V., Cicerone, R.J., Singh, H.B., Kiehl, J.T., 1985. Trace gas trends and their potential role in climate change. Journal of Geophysical Research: Atmospheres, 90(D3), 5547-5566.

Saltzman, B.E. and Gilbert, N., 1959. Iodometric microdetermination of organic oxidants and ozone. Resolution of mixtures by kinetic colorimetry. Analytical Chemistry, 31(11), 1914-1920.

Schnadt Poberaj, C., Staehelin, J., Brunner, D., Thouret, V., Mohnen, V., 2007. A UT/LS ozone climatology of the nineteen seventies deduced from the GASP aircraft measurement program. Atmospheric Chemistry and Physics, 7(22), 5917-5936.

Schultz, M.G., Schröder, S., Lyapina, O., Cooper, O.R., Galbally, I., Petropavlovskikh, I., Von Schneidemesser, E., Tanimoto, H., Elshorbany, Y., Naja, M., Seguel, R.J., 2017. Tropospheric Ozone Assessment Report: Database and metrics data of global surface ozone observations. Elementa: Science of the Anthropocene, 5.

Sharma, S., Sharma, P., Khare, M., 2017. Photo-chemical transport modelling of tropospheric ozone: A review. Atmospheric Environment, 159, 34-54.

Smit, H.G.J., Sträter, W., Helten, M., Kley, D., Ciupa, D., Claude, H.J., Köhler, U., Hoegger, B., Levrat, G., Johnson, B., Oltmans, S.J., Kerr, J.B., Tarasick, D.W., Davies, J., Shitamichi, M., Srivastav, S.K., Vialle, C., 1996. JOSIE: The 1996 WMO international intercomparison of ozonesondes under quasi-flight conditions in the environmental chamber at Jülich, *Proc. Quadrennial Ozone Symposium 1996*, *l'Aquila, Italy,* edited by R. D. Bojkov and G. Visconti, pp. 971-974, Parco Sci. e Tecnol. d'Abruzzo, Italy, 1996.

Smit, H.G., Straeter, W., Johnson, B.J., Oltmans, S.J., Davies, J., Tarasick, D.W., Hoegger, B., Stubi, R., Schmidlin, F.J., Northam, T., Thompson, A.M., 2007. Assessment of the performance of ECC-ozonesondes under quasi-flight conditions in the environmental simulation chamber: Insights from the Juelich Ozone Sonde Intercomparison Experiment (JOSIE). Journal of Geophysical Research: Atmospheres, 112(D19), D19306, doi:10.1029/2006JD007308.

Smit, H.G.J., 2014. Ozonesondes, in Encyclopedia of Atmospheric Sciences, Second Edition, edited by G.R. North, J.A. Pyle, and F. Zhang, Vol 1, pp. 372–378, Academic Press, London.

Smit, H. G. J., Poyraz, D., Van Malderen, R., Thompson, A. M., Tarasick, D. W., Stauffer, R. M.,

610 Johnson, B. J., and Kollonige, D. E., 2024. New insights from the Jülich Ozone Sonde
611 Intercomparison Experiment: calibration functions traceable to one ozone reference instrument.
612 Atmospheric Measurement Techniques, 17, 73–112, https://doi.org/10.5194/amt-17-73-2024.
613 Smit, H.G.J., Thompson, A.M., and the ASOPOS 2.0 Panel, 2021. Ozonesonde Measurement
614 Principles and 1300 Best Operational Practices, WMO Global Atmosphere Watch Report
615 Series, No. 268, World Meteorological Organization, 1301 Geneva, [Available online at
616 https://library.wmo.int/doc_num.php?explnum_id=10884].
617 Solomon, S., 1999. Stratospheric ozone depletion: A review of concepts and history. Reviews of
618 Geophysics, 37(3), 275-316.
619 Staehelin, J., Harris, N.R., Appenzeller, C. and Eberhard, J., 2001. Ozone trends: A review. Reviews
620 of Geophysics, 39(2), 231-290.
621 Staufer, J., Staehelin, J., Stübi, R., Peter, T., Tummon, F., Thouret, V., 2013. Trajectory matching of
622 ozonesondes and MOZAIC measurements in the UTLS - Part 1: Method description and
623 application at Payerne, Switzerland. Atmospheric Measurement Techniques, 6, 3393-3406.
624 doi:10.5194/amt-6-3393-2013.
625 Staufer, J., Staehelin, J., Stübi, R., Peter, T., Tummon, F., Thouret, V., 2014. Trajectory matching of
626 ozonesondes and MOZAIC measurements in the UTLS - Part 2: Application to the global
627 ozonesonde network. Atmospheric Measurement Techniques, 7, 241-266. doi:10.5194/amt-7-
628 241-2014.
629 Stübi, R., Levrat, G., Hoegger, B., Viatte, P., Staehelin, J., Schmidlin, F.J., 2008. In-flight
630 comparison of Brewer-Mast and electrochemical concentration cell ozonesondes. Journal of
631 Geophysical Research: Atmospheres, 113(D13). https://doi.org/10.1029/2007JD009091.
632 Tanimoto, H., Zbinden, R.M., Thouret, V., Nédélec, P., 2015. Consistency of tropospheric ozone
633 observations made by different platforms and techniques in the global databases. Tellus B:
634 Chemical and Physical Meteorology, 67(1), 27073.
635 Tarasick, D. W., Davies, J., Anlauf, K., Watt, M., Steinbrecht, W., Claude, H. J., 2002. Laboratory
636 investigations of the response of Brewer-Mast ozonesondes to tropospheric ozone. Journal of
637 Geophysical Research: Atmospheres, 107(D16), ACH-14,
638 https://doi.org/10.1029/2001JD001167.

Tarasick, D. W., Davies, J., Smit, H. G., Oltmans, S. J., 2016. A re-evaluated Canadian ozonesonde record: measurements of the vertical distribution of ozone over Canada from 1966 to 2013. Atmospheric Measurement Techniques, 9(1), 195-214.

Tarasick, D.W., Galbally, I., Cooper, O.R., Schultz, M.G., Ancellet, G., LeBlanc, T., Wallington, T.J., Ziemke, J., Liu, X., Steinbacher, M., Stähelin, J., Vigouroux, C., Hannigan, J., García, O., Foret, G., Zanis, P., Weatherhead, E., Petropavlovskikh, I., Worden, H., Neu, J.L., Osman, M., Liu, J., Lin, M., Granados-Muñoz, M., Thompson, A.M., Oltmans, S.J., Cuesta, J., Dufour, G., Thouret, V., Hassler, B., Thompson, A.M., Trickl, T., 2019. TOAR- Observations: Tropospheric ozone from 1877 to 2016, observed levels, trends and uncertainties. Elementa: Science of the Anthropocene, 7(1), 39. DOI: http://doi.org/10.1525/elementa.376.

Tarasick, D.W., Smit, H.G., Thompson, A.M., Morris, G.A., Witte, J.C., Davies, J., Nakano, T., Van Malderen, R., Stauffer, R.M., Johnson, B.J., Stübi, R., Oltmans, S.J., Vömel, H., 2021. Improving ECC ozonesonde data quality: Assessment of current methods and outstanding issues. Earth and Space Science, 8, e2019EA000914. https://doi.org/10.1029/2019EA000914.

Thouret, V., Clark, H., Petzold, A., Nédélec, P., Zahn, A., 2022. IAGOS: Monitoring Atmospheric Composition for Air Quality and Climate by Passenger Aircraft. In Handbook of Air Quality and Climate Change (pp. 1-14). Singapore: Springer Nature Singapore.

Thouret, V., Marenco, A., Logan, J.A., Nédélec, P., Grouhel, C., 1998. Comparisons of ozone measurements from the MOZAIC airborne program and the ozone sounding network at eight locations. Journal of Geophysical Research: Atmospheres, 103(D19), 25695-25720. doi: 10.1029/98JD02243.

Thompson, A. M., Smit, H. G. J., Witte, J. C., Stauffer, R. M., Johnson, B. J., Morris, G., von der Gathen, P., Van Malderen, R., Davies, J., Piters, A., Allaart, M., Posny, F., Kivi, R., Cullis, P., Hoang Anh, N. T., Corrales, E., Machinini, T., da Silva, F. R., Paiman, G., Thiong'o, K., Zainal, Z., Brothers, G. B., Wolff, K. R., Nakano, T., Stübi, R., Romanens, G., Coetzee, G. J. R., Diaz, J. A., Mitro, S., Mohamad, M., Ogino, S., 2019. Ozonesonde quality assurance: The JOSIE-SHADOZ (2017) experience. Bulletin of the American Meteorological Society, 100(1), 155-171.

Vingarzan, R., 2004. A review of surface ozone background levels and trends. Atmospheric

668 Environment, 38(21), 3431-3442.
669 Vömel, H., Smit, H. G. J., Tarasick, D., Johnson, B., Oltmans, S. J., Selkirk, H., Thompson, A. M.,
670 Stauffer, R. M., Witte, J. C., Davies, J., van Malderen, R., Morris, G. A., Nakano, T., Stübi, R.,
671 2020. A new method to correct the electrochemical concentration cell (ECC) ozonesonde time
672 response and its implications for "background current" and pump efficiency, Atmospheric
673 Measurement Techniques, 13, 5667-5680, https://doi.org/10.5194/amt-13-5667-2020.
674 Wang, H., Ke, Y., Tan, Y., Zhu, B., Zhao, T., Yin, Y., 2023. Observational evidence for the dual roles
675 of BC in the megacity of eastern China: Enhanced O_3 and decreased $PM_{2.5}$
676 pollution. Chemosphere, 327, 138548.
677 Wang, H., Lu, X., Jacob, D.J., Cooper, O.R., Chang, K.L., Li, K., Gao, M., Liu, Y., Sheng, B., Wu, K.,
678 Wu, T., 2022. Global tropospheric ozone trends, attributions, and radiative impacts in 1995-2017:
679 an integrated analysis using aircraft (IAGOS) observations, ozonesonde, and multi-decadal
680 chemical model simulations. Atmospheric Chemistry and Physics, 22(20), 13753-13782.
681 Wang, T., Xue, L., Brimblecombe, P., Lam, Y.F., Li, L., Zhang, L., 2017. Ozone pollution in China:
682 A review of concentrations, meteorological influences, chemical precursors, and
683 effects. Science of the Total Environment, 575, 1582-1596.
684 Williamson, C.E., Neale, P.J., Hylander, S., Rose, K.C., Figueroa, F.L., Robinson, S.A., Häder, D.P.,
685 Wängberg, S.Å., Worrest, R.C., 2019. The interactive effects of stratospheric ozone depletion,
686 UV radiation, and climate change on aquatic ecosystems. Photochemical and Photobiological
687 Sciences, 18(3), 717-746.
688 Xu, J., Huang, X., Wang, N., Li, Y., Ding, A., 2021. Understanding ozone pollution in the Yangtze
689 River Delta of eastern China from the perspective of diurnal cycles. Science of the Total
690 Environment, 752, 141928.
691 Yang, T., Li, H., Wang, H., Sun, Y., Chen, X., Wang, F., Xu, L., Wang, Z., 2023. Vertical aerosol
692 data assimilation technology and application based on satellite and ground lidar: A review and
693 outlook. Journal of Environmental Sciences, 123, 292-305.
694 Young, P.J., Naik, V., Fiore, A.M., Gaudel, A., Guo, J., Lin, M.Y., Neu, J.L., Parrish, D.D., Rieder,
695 H.E., Schnell, J.L., Tilmes, S., 2018. Tropospheric Ozone Assessment Report: Assessment of
696 global-scale model performance for global and regional ozone distributions, variability, and

trends. Elementa: Science of the Anthropocene, 6.

Yu, R., Lin, Y., Zou, J., Dan, Y., Cheng, C., 2021. Review on atmospheric Ozone pollution in China: Formation, spatiotemporal distribution, precursors and affecting factors. Atmosphere, 12(12), 1675.

Zang, Z., Liu, J., Tarasick, D., Moeini, O., Bian, J., Zhang, J., Thompson, A. M., Van Malderen, R., Smit, H. G. J., Stauffer, R. M., Johnson, B. J., Kollonige, D. E., 2024. An improved Trajectory-mapped Ozonesonde dataset for the Stratosphere and Troposphere (TOST): update, validation and applications, EGUsphere [preprint], https://doi.org/10.5194/egusphere-2024-800, 2024.

Zbinden, R.M., Thouret, V., Ricaud, P., Carminati, F., Cammas, J.P., Nédélec, P., 2013. Climatology of pure tropospheric profiles and column contents of ozone and carbon monoxide using MOZAIC in the mid-northern latitudes (24° N to 50° N) from 1994 to 2009. Atmospheric Chemistry and Physics, 13(24), 12363-12388, https://doi.org/10.5194/acp-13-12363-2013, 2013.

Zhang, L., Jacob, D.J., Boersma, K.F., Jaffe, D.A., Olson, J.R., Bowman, K.W., Worden, J.R., Thompson, A.M., Avery, M.A., Cohen, R.C., Dibb, J.E., 2008. Transpacific transport of ozone pollution and the effect of recent Asian emission increases on air quality in North America: an integrated analysis using satellite, aircraft, ozonesonde, and surface observations. Atmospheric Chemistry and Physics, 8(20), 6117-6136.

Zhao, K., Huang, J., Wu, Y., Yuan, Z., Wang, Y., Li, Y., Ma, X., Liu, X., Ma, W., Wang, Y., Zhang, X., 2021. Impact of stratospheric intrusions on ozone enhancement in the lower troposphere and implication to air quality in Hong Kong and other South China regions. Journal of Geophysical Research: Atmospheres, 126(18), e2020JD033955.

Figures

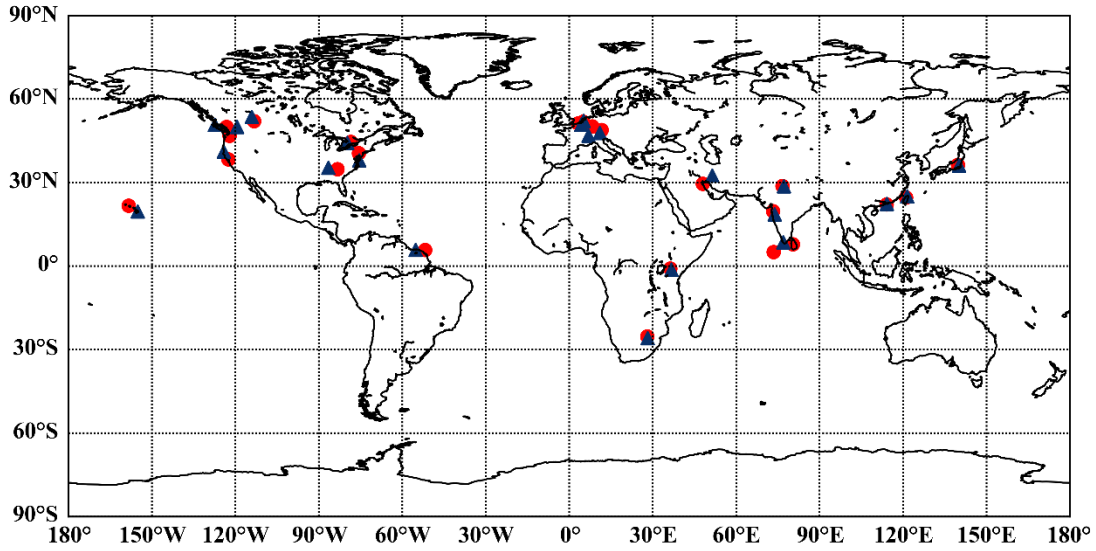

Figure 1. Map of 23 pairs of sites used in this study. Red circle markers are IAGOS sites, blue triangle markers are WOUDC sites.

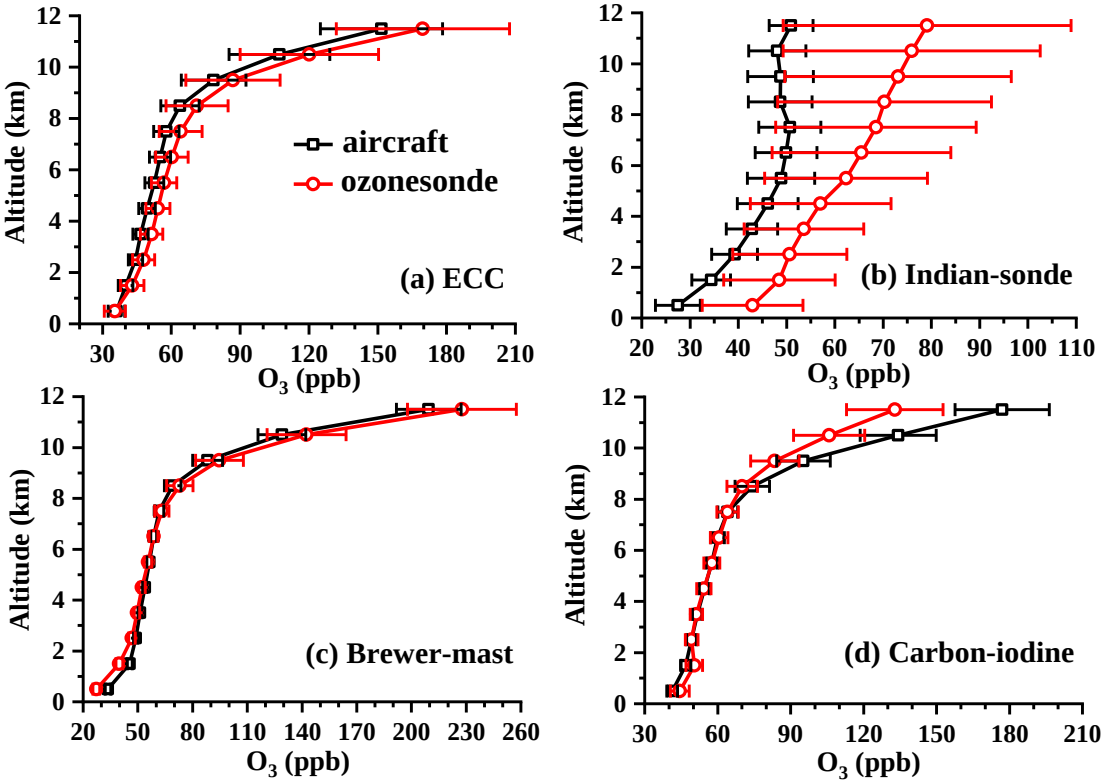

Figure 2. Comparison of the vertical profiles of tropospheric O_3 observed between aircraft measurements and four types of ozonesondes, ECC, Indian-sonde, Brewer-mast, and Carbon-iodine. The error bar length is 4 times the standard error (SE) of the mean (equivalent to 95% confidence limits on the averages).

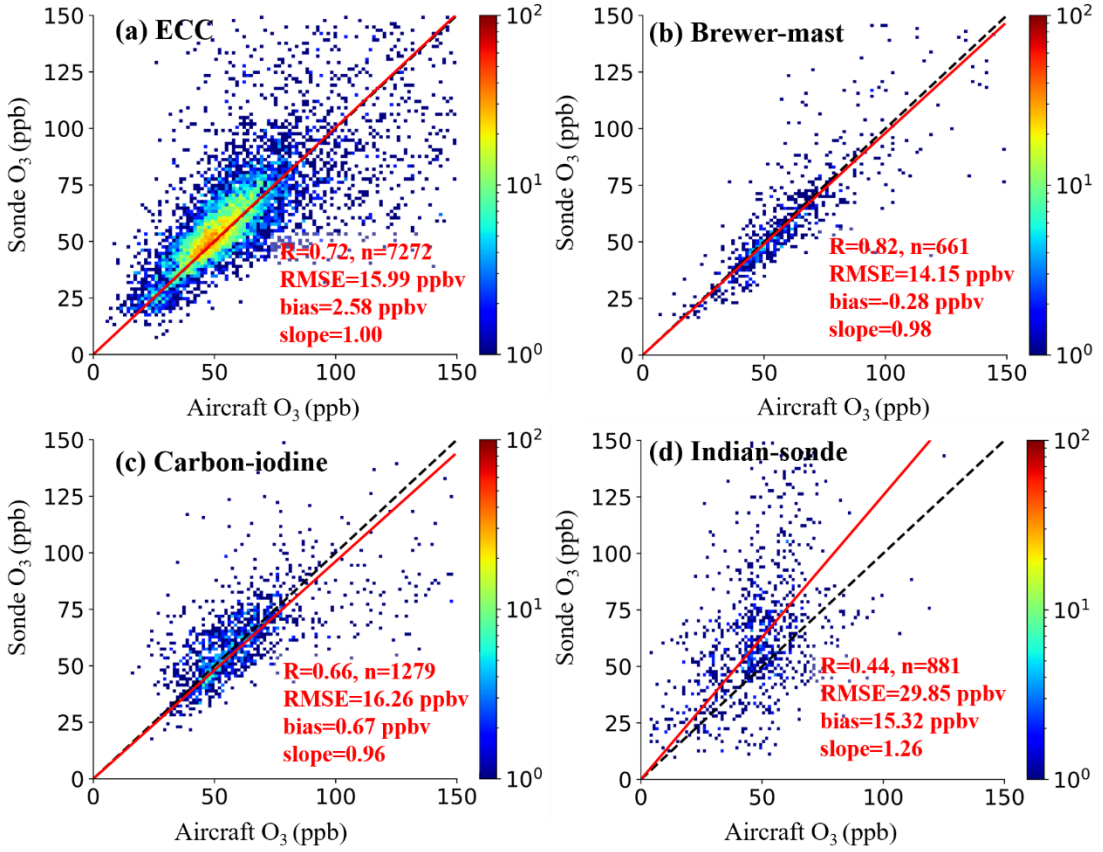

Figure 3. Correlation (*R*) of monthly mean ozone mixing ratios between ozonesonde and aircraft measurements. While IAGOS does measure in the lower stratosphere these values are usually far from the airport, so the sonde-aircraft distance will be large, we only plots data below 150 ppb. The black dashed line shows the 1:1 axis, the red line shows the linear fit (with the intercept set to 0), the color bar shows the data counts. Correlations are significant at the 99% level (p <0.01). *N* denotes the number of data points, R is the correlation coefficient, Bias is the overall average difference in monthly mean values [Ozonesonde ozone – Aircraft ozone, in ppb], RMSE is the root mean square error, slope is the slope of the linear fit line. All data points are based on the monthly mean.

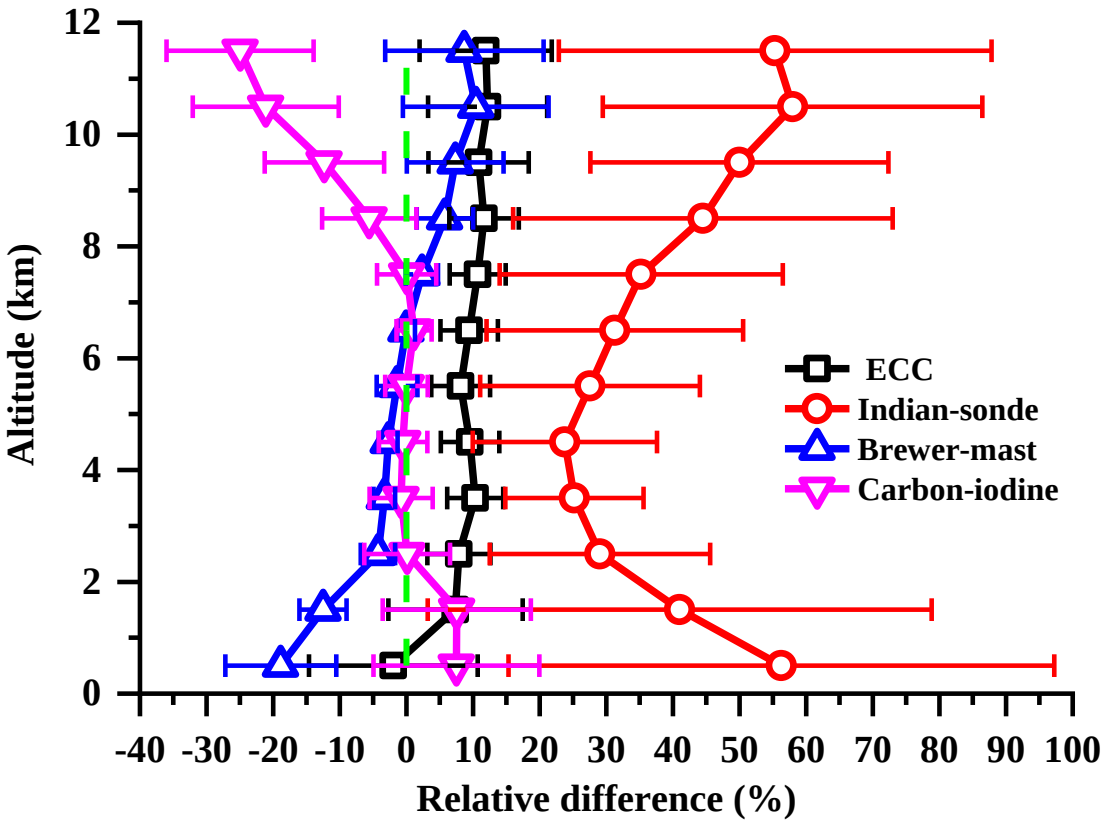

Figure 4. Mean relative difference (RD) between the ozonesonde O_3 and aircraft O_3 data. RD is calculated from ($O_{3\text{-ozonesonde}}$ - $O_{3\text{-aircraft}}$)/ $O_{3\text{-aircraft}}$×100%. The green dashed line is the zero line.

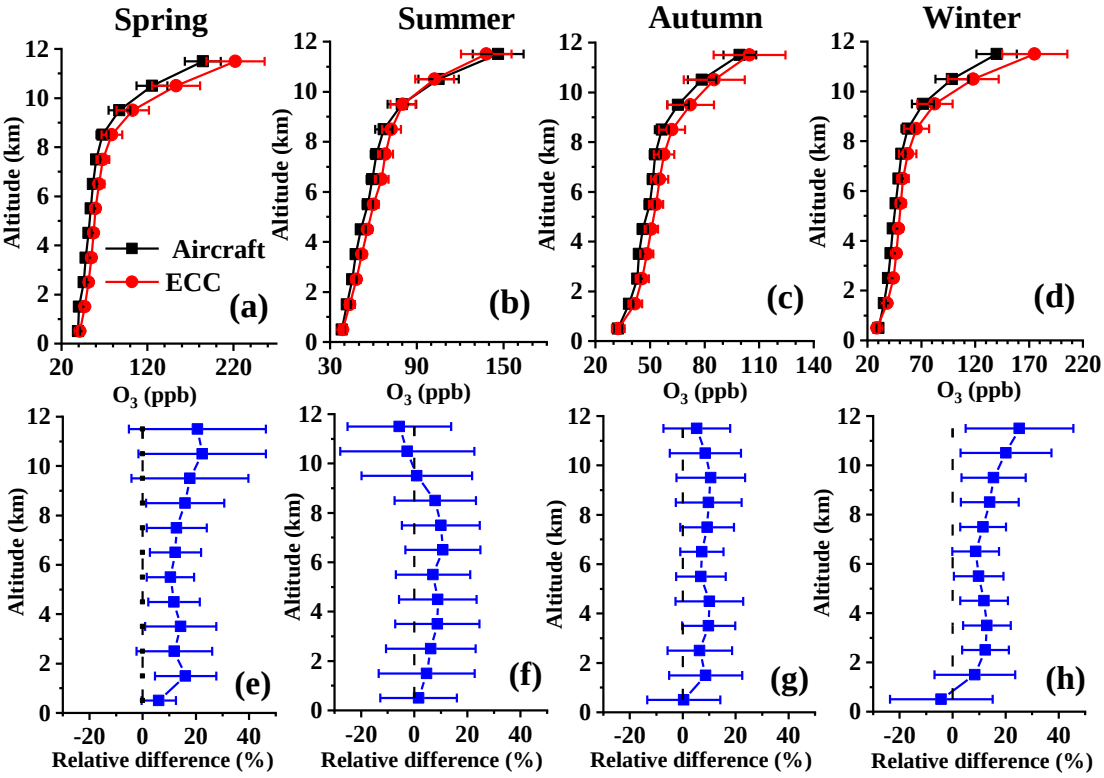

Figure 5. The mean difference in vertical profiles of the tropospheric O_3 between ECC ozonesonde and aircraft observations in four seasons (a-d) and their mean relative difference, the black dashed line is the zero line (e-h).

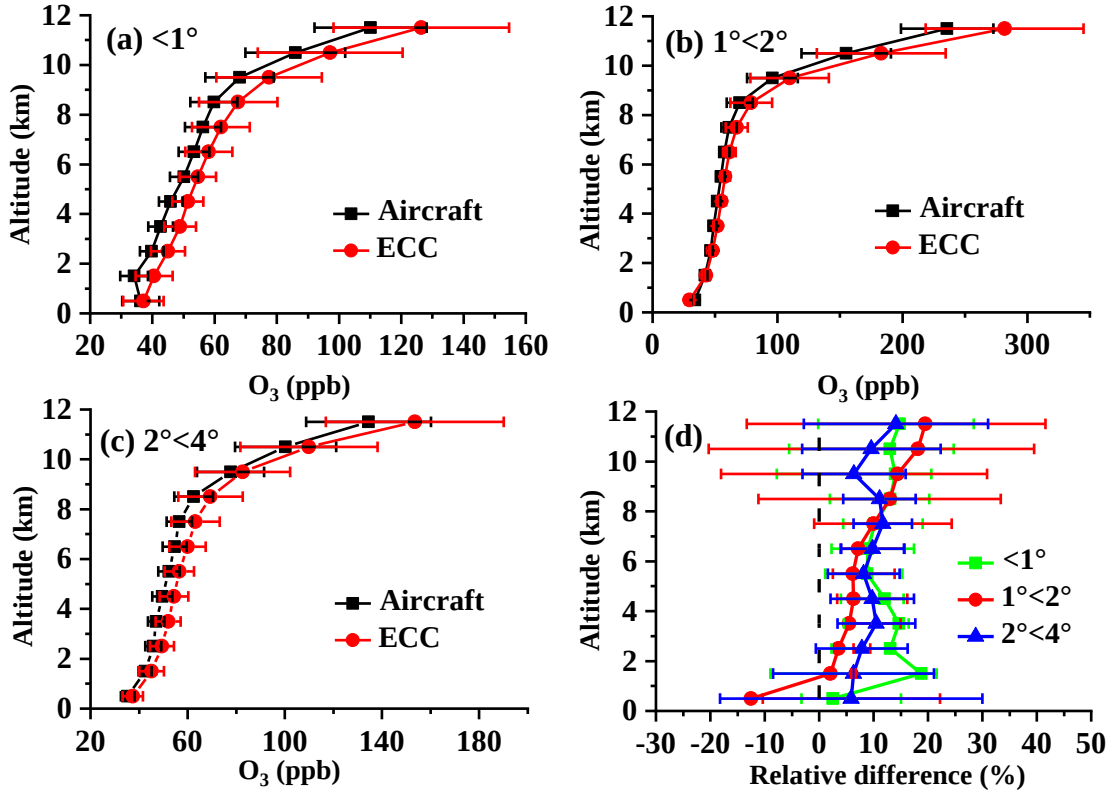

Figure 6. The annual mean vertical profiles of tropospheric O_3 between ECC ozonesonde and aircraft observations at station-pair distances (D) of D<1° (a), 1°< D <2° (b), and 2°< D <4°. The relative differences for the three categories are shown in (d), the black dashed line is the zero line.

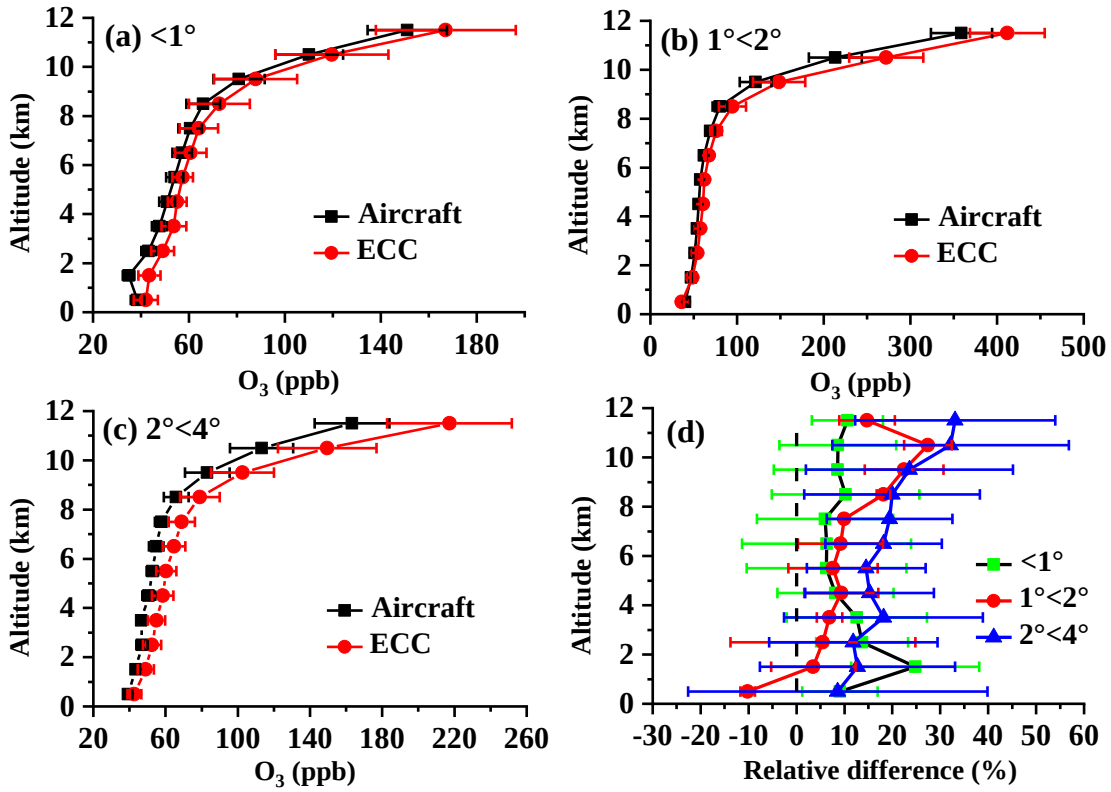

Figure 7. The seasonal mean vertical profiles of tropospheric O_3 in spring between ECC ozonesonde and aircraft observations at station-pair distances (D) of D<1° (a), 1°< D <2° (b), and 2°< D <4°.The relative differences for the three categories are shown in (d), the black dashed line is the zero line.

Tables

Table 1. Summary of the station information, including station's name, geolocation, the number of profiles, observational period, and the station-pair distance used in this study.

MOZAIC-IAGOS				WOUDC					Station- airport distance (km)	No. valid data months	observation period
Station name	Lon	Lat	No. profiles	Station name	Lon	Lat	No. profiles	Type			
Toronto	-78.50	44.58	321	Egbert	-79.78	44.23	181	ECC	108.87	33	2004-2008
Dusseldorf	4.96	51.82	412	De Bilt	5.18	52.10	333	ECC	34.59	63	1995-2013
Munich	11.78	48.35	2136	Hohenpeissenberg	11.02	47.81	1032	Brewer-mast	82.42	67	1996-2006
Johannesburg	28.07	-25.32	199	Irene	28.22	-25.91	135	ECC	67.30	26	1998-2003
Nairobi	36.33	-0.94	114	Nairobi	36.75	-1.30	42	ECC	61.50	10	1997-1998
Mumbai	73.26	19.05	122	Pune	73.85	18.53	56	Indian-sonde	84.85	35	1996-2003
Delhi	76.65	28.73	342	New Delhi	77.18	28.63	88	Indian-sonde	52.88	50	1995-2016
Hongkong	114.11	22.10	123	King's Park	114.17	22.31	115	ECC	24.15	25	2000-2005
Taipei	121.08	24.59	2115	Taipei	121.48	25.02	58	ECC	62.58	31	2014-2018
Tokyo	139.73	36.33	1342	Tateno (Tsukuba)	140.13	36.05	655	Carbon-iodine	47.52	116	1995-2006

Calgary	-113.25	52.03	170	Edmonton	-114.10	53.55	112	ECC	178.41	17	2009-2011
Brussels	3.24	51.21	2412	Uccle	4.36	50.80	736	ECC	148.40	55	1997-2009
Honolulu	-158.33	21.66	169	Hilo (HI)	-155.07	19.58	107	ECC	410.56	16	2015-2017
Vancouver	-123.14	49.95	595	Kelowna	-127.38	50.69	594	ECC	312.01	68	2003-2015
San-Francisco	-122.50	38.30	34	Trinidad Head (CA)	-124.15	41.05	53	ECC	336.78	10	1999-2001
Portland	-122.06	46.76	385	Kelowna	-119.38	49.97	317	ECC	408.08	45	2003-2009
Atlanta	-83.28	34.78	34	Huntsville (AL)	-86.58	35.28	85	ECC	305.54	10	1999-2006
Washington	-75.59	40.52	610	Wallops Island (VA)	-75.46	37.94	616	ECC	287.09	80	1994-2014
Cayenne	-51.78	5.75	200	Paramaribo	-55.21	5.81	64	ECC	379.50	9	2002-2013
Frankfurt	8.30	50.16	12742	Payerne	6.94	46.81	2673	ECC	385.72	204	2002-2020
Kuwait-City	48.01	29.52	105	Esfahan	51.43	32.48	34	ECC	463.15	17	2001-2004
Male	73.51	5.00	76	Trivandrum	76.95	8.48	45	Indian-sonde	543.73	24	1997-2000
Colombo	80.41	7.79	31	Trivandrum	76.95	8.48	37	Indian-sonde	388.49	11	1998-2000

Table 2. Bias, correlation coefficient (R), and RMSE for four types of ozonesonde and aircraft observations in four seasons.

Type	Season	Bias ($O_{3\text{-ozonesonde}}$ - $O_{3\text{-aircraft}}$) (ppb)	R	RMSE (ppb)
ECC	Spring	17.34	0.76	65.52
	Summer	1.96	0.76	40.15
	Autumn	1.75	0.71	34.47
	Winter	7.61	0.71	51.74
Brewer-mast	Spring	10.22	0.94	43.51
	Summer	2.99	0.83	48.79
	Autumn	6.53	0.79	29.40
	Winter	6.11	0.88	45.45
Carbon-iodine	Spring	-9.19	0.84	38.34
	Summer	3.83	0.46	29.31
	Autumn	2.33	0.68	15.10
	Winter	-16.68	0.88	44.72
Indian-sonde	Spring	19.64	0.44	44.30
	Summer	19.58	0.57	37.44
	Autumn	20.38	0.45	37.30
	Winter	40.07	0.18	64.99

Table 3. Bias, correlation coefficient(R) and RMSE for ECC and Indian-sonde ozonesonde and aircraft observations at different station-airport distances.

Type	Station-pair distance	Bias ($O_{3\text{-ozonesonde}}$ - $O_{3\text{-aircraft}}$) (ppb)	R	RMSE (ppb)
ECC	<1°	9.78	0.78	47.46
	1°-2°	8.91	0.90	40.73
	2°-4°	5.65	0.67	51.00
Indian-sonde	<1°	26.71	0.37	49.54
	2°-4°	15.35	0.24	30.86

Table 4. Comparison of the sondes of each type to IAGOS. (average ± 2 times the standard error (SE)) Indian-sonde/ECC is (Indian-sonde/IAGOS)/(ECC/IAGOS), Brewer-mast/ECC is (Brewer-mast/IAGOS)/(ECC/IAGOS), Carbon-iodine/ECC is (Carbon-iodine /IAGOS)/(ECC/IAGOS)

Altitude(km)	Indian-sonde/ECC	Brewer-mast/ECC	Carbon-iodine/ECC	ECC/ IAGOS
0-1	1.59 ±1.74	0.83 ±0.96	1.10 ±1.36	0.98 ±1.28
1-2	1.31 ±1.83	0.81 ±0.90	1.00 ±1.05	1.07 ±1.58
2-3	1.20 ±1.62	0.89 ±0.97	0.93 ±0.85	1.08 ±1.54
3-4	1.14 ±1.57	0.88 ±0.94	0.90 ±0.87	1.10 ±1.48
4-5	1.13 ±1.61	0.89 ±1.02	0.91 ±0.99	1.10 ±1.44
5-6	1.18 ±1.76	0.91 ±1.05	0.92 ±1.04	1.08 ±1.37
6-7	1.20 ±1.89	0.91 ±1.00	0.92 ±0.82	1.09 ±1.54
7-8	1.22 ±1.92	0.92 ±0.94	0.90 ±0.64	1.11 ±1.69
8-9	1.29 ±2.09	0.95 ±0.99	0.85 ±0.55	1.12 ±1.61
9-10	1.35 ±2.35	0.97 ±1.09	0.79 ±0.62	1.11 ±1.46
10-11	1.41 ±3.26	0.98 ±1.21	0.70 ±0.68	1.12 ±1.37
11-12	1.39 ±4.61	0.97 ±1.19	0.67 ±0.72	1.12 ±1.42